J Biol Inorg Chem (2002) 7: 551–559
DOI 10.1007/s00775-001-0336-9

ORIGINAL ARTICLE

Laura S. Busenlehner · Julius L. Apuy
David P. Giedroc

Characterization of a metalloregulatory bismuth(III) site in *Staphylococcus aureus* pI258 CadC repressor

Received: 23 July 2001 / Accepted: 19 December 2001 / Published online: 8 February 2002

Abstract *Staphylococcus aureus* pI258 CadC is a metal sensor protein that regulates the expression of the *cad* operon which encodes metal ion resistance proteins involved in the efficient efflux of Cd(II), Pb(II), Zn(II) and, according to one report , Bi(III) ions. In this paper, direct evidence is presented that Bi(III) binds to CadC and negatively regulates *cad* operator/promoter (O/P) binding. Optical absorption spectroscopy reveals that dimeric CadC binds ~0.8 mol equivalents of Bi(III) per CadC monomer to form a coordination complex characterized by three $S^- \rightarrow Bi(III)$ ligand-to-metal charge transfer transitions, with the longest wavelength absorption band centered at 415 nm ($\epsilon_{415} = 4000\ M_{Bi}^{-1}\ cm^{-1}$). UV-Vis absorption spectra of wild-type and mutant Cys→Gly (Ser) substitution CadC mutants compared to $[Bi(DTT)_2]$, $[Bi(GSH)_3]$ and $[Bi(NAC)]_3$ model complexes reveal that Cys7, Cys11, Cys60 and Cys58 directly coordinate Bi(III) in a tetrathiolate coordination complex. The apparent affinity derived from a Bi(III)-displacement optical titration with Cd(II) is estimated to be $K_{Bi} \leq 10^{12}\ M^{-1}$. Apo-CadC binds with high affinity [$K_a = 1.1(\pm 0.3) \times 10^9\ M^{-1}$; 0.40 M NaCl, pH 7.0, 25 °C] to a 5′-fluorescein-labeled *cad* O/P oligonucleotide ,while the binding of one molar equivalent of Bi(III) per CadC monomer (Bi_1-CadC) reduces the affinity by ~170-fold. Strikingly, Bi(III)-responsive negative regulation of *cad* O/P binding is abrogated for Bi_1-C60G CadC and severely disrupted in Bi_1-C7G CadC, whose relative affinity is reduced only 10-fold. The mechanism of Bi(III)-responsive metalloregulation is discussed, based on the findings presented here. Electronic supplementary material to this paper can be obtained by using the Springer Link server located at http://dx.doi.org/10.1007/s00775-001-0336-9.

Keywords Bismuth · CadC · Optical absorption spectroscopy · Metal ion resistance · Cadmium

Abbreviations *Bi_1*: one equivalent of Bi · *Bis-Tris*: bis(2-hydroxyethyl)iminotris(hydroxymethyl)methane · *DTNB*: 5,5′-dithiobis(2-nitrobenzoic acid) · *DTT*: dithiothreitol · *GSH*: reduced glutathione · *LMCT*: ligand-to-metal charge transfer · *NAC*: *N*-acetylcysteine · *O/P*: operator/promoter

Introduction

Bismuth(III) salts have long been known to be toxic to bacteria, particularly *Heliobacter pylori*, which thrives in an acidic environment in the gut where it causes a variety of gastrointestinal disorders [1]. The enzyme urease is critical to the survival of *H. pylori*, which generates ammonia used to neutralize the surrounding milieu; Bi(III) salts kill *H. pylori*, presumably by substituting for one or both of the Ni(II) ions in the binuclear Ni(II) active site, leading to urease inactivation. The inactivation of other metalloenzymes by Bi(III) substitution, including alcohol dehydrogenase, may play at least some role in this process for this and other organisms [1, 2, 3]. In mammalian cells, Bi(III) is a potent inducer of the expression of the intracellular chelator metallothionein [4], and it has been demonstrated that mammalian metallothioneins bind Bi(III) tightly in trigonal S_3 coordination complexes [5]. Bi(III) also binds tightly to serum transferrin, blocking the essential iron transport function of this protein [6].

In response to environmental stress mediated by toxic metal ions, chromosomal and/or plasmid-encoded heavy metal resistance/detoxification systems have evolved in

Electronic supplementary material to this paper can be obtained by using the Springer Link server located at http://dx.doi.org/10.1007/s00775-001-0336-9

L.S. Busenlehner · J.L. Apuy · D.P. Giedroc (✉)
Department of Biochemistry and Biophysics,
Center for Advanced Biomolecular Research,
Texas A&M University,
College Station, TX 77843-2128, USA
E-mail: giedroc@tamu.edu
Tel.: +1-979-8454231
Fax: +1-979-8624718

most, if not all, bacteria for many environmental pollutants, including Cd(II), Pb(II) and As(III) [7, 8, 9]. Many of these systems are composed of a single transcriptionally regulated operon which encodes two genes: (1) a transcriptional repressor or metal sensor protein which regulates the expression of the operon in response to a change in the intracellular concentration of specific metal ion, and (2) a resistance protein, such as a specific efflux pump, an intracellular chelator, e.g. a metallothionein, or a metal ion reductase [10]. The *cad* operon encoded on plasmid pI258 of *Staphylococcus aureus* is an example of a resistance system which responds to Cd(II), Pb(II), Zn(II) and possibly Bi(III) [7]. The *cad* operon is composed of two genes: one that encodes CadC, the metal-responsive transcriptional repressor or metal sensor, and a second that encodes CadA, a Cd(II)- and Pb(II)-specific P-type ATPase efflux pump [8, 11].

It was recently demonstrated with a variety of spectroscopic techniques that CadC, a member of the ArsR/SmtB family of metal responsive transcriptional repressors, binds Cd(II) and Pb(II) with high affinity. The spectroscopic data are most consistent with a coordination complex composed of three cysteine thiolate ligands to Pb(II) or four cysteine thiolate ligands to Cd(II) ([12]; Busenlehner L, Giedroc DP, manuscript in preparation). The binding of either stoichiometric Cd(II) or Pb(II) to CadC results in a significant decrease in affinity for the *cad* operator/promoter (O/P) in vitro, consistent with a model in which the mechanism of derepression in vivo lies at the level of negative regulation of DNA binding by bound inducer ions. In vivo β-lactamase assays described by Yoon et al. [7] show that Bi(III) was among the strongest inducers of the *cadA-blaZ* fusion system in the native host *S. aureus*, while Rensing et al. [8] reported no induction with Bi(III) in a similar experiment conducted in *Escherichia coli*. Gel mobility shift assays also suggested that Bi(III) was at least partly capable of dissociating bound apo-CadC from the *cad* O/P [11].

Bi(III) is classified as a borderline metal ion according to the hard-soft acid-base theory [13], meaning that Bi(III) binds both hard protein ligands such as carboxylate oxygens and imidazole nitrogens as well as soft ligands like cysteine sulfurs, the latter of which is presumed to be the preferred ligand for the ion in vivo (for a review, see [1]). Bi(III) coordination chemistry is thought to be quite similar to that of Pb(II); both ions contain a $6s^2$ lone pair of electrons, possess similar ionic radii (1.03 Å for Bi^{3+} and 1.1 Å for Pb^{2+}) and are known to form thermodynamically stable, but kinetically labile, complexes with thiolate sulfur atoms [1]. Since CadC was recently shown to bind Pb(II) via cysteine thiolate ligands [12], Bi(III) might also bind to a site which is identical or partially overlapping that of Pb(II) and Cd(II); however, it seemed possible that the Bi(III) binding might not lead to negative regulation of *cad* O/P binding of CadC [12]. In this report, optical absorption spectroscopy and fluorescence anisotropy are employed to determine if Bi(III) binds directly to CadC and, if so, whether or not metal binding allosterically regulates *cad* O/P binding. Our findings reveal that each CadC monomer within homodimeric CadC binds ~0.8 mol equivalents Bi(III) with a wild-type coordination complex of high affinity composed of four cysteine thiolate ligands. In addition, CadC with one equivalent of Bi(III) per monomer is characterized by a significantly decreased affinity for the *cad* O/P oligonucleotide as monitored by fluorescence anisotropy titrations, which predicts a role for CadC in Bi(III) resistance in *S. aureus* in vivo.

Materials and methods

Chemicals

All buffers were prepared using Milli-Q doubly distilled, deionized water and metals were removed from all solutions by passage over a Chelex-100 column. MES and Bis-Tris buffer salts, EDTA, ampicillin, kanamycin, chloramphenicol and 5,5′-dithiobis(2-nitrobenzoic acid) (DTNB) were purchased from Sigma. Chelex-100 resin was obtained from Bio-Rad. Ultrapure bismuth(III) nitrate and cadmium(II) chloride were purchased from Johnson Matthey. Reduced glutathione (γ-L-Glu-Cys-Gly; GSH) and *N*-acetylcysteine (NAC) were obtained from Sigma, while dithiothreitol (DTT) was acquired from Acros.

Purification of wild-type CadC and mutants

The construction of *pET-CadC* and the purification of wild-type CadC by polyethyleneimine (PEI) precipitation, ammonium sulfate precipitation, cation exchange chromatography, and size exclusion chromatography have been described [12]. The construction of the *pMW1* series of plasmids, which direct the overexpression of cysteine substitution mutants (Cys→Gly/Ser) of CadC, has also been reported [14] and were purified using a procedure based on the protocol for wild-type CadC. Inspection of overloaded Coomassie-stained Tricine-SDS gels revealed that the purity of all proteins was ~95%. The concentration of purified wild-type CadC and the cysteine-substitution mutants was determined from the calculated molar extinction coefficient of 6585 M^{-1} cm^{-1} [15].

Atomic absorption spectroscopy

The Zn(II) content of all preparations of CadC was determined using a Perkin-Elmer AAnalyst 700 atomic absorption spectrophotometer operating in flame mode using a Zn(II) hollow cathode lamp. Zn(II) was detected at 213.9 nm with a slit width of 0.7 nm. The total metal content of all preparations of purified, "metal-free" CadC (wild-type and cysteine-substitution mutants) was no more than 0.03 mol of Zn(II) per mol of CadC monomer. For the determination of the concentration of Bi(III) used for titrant stocks for optical titrations, Bi(III) was detected with a Bi(III) hollow cathode lamp set at 223.1 nm with a slit width of 0.2 nm. The Cd(II) concentration for displacement titrations was determined with a Cd(II)-specific hollow cathode lamp detecting at 228.8 nm with a slit width of 0.7 nm.

Free thiol quantification

A standard DTNB assay was used to determine the number of free thiols for each of the CadC proteins [16]. In an anaerobic glovebox, 45 μL of 2.5 mM DTNB solution (0.25 mM DTNB final) was added to 20 μM CadC in 400 μL of buffer S (50 mM MES, 0.40 M NaCl, pH 7.0). The mixture was incubated for 30 min to ensure

that the reaction was complete. After subtracting the absorbance of the buffer with same amount of DTNB, the molar concentration of thiolate anion was quantified at 412 nm ($\epsilon_{412} = 13{,}600\ M^{-1}\ cm^{-1}$). Wild-type CadC, which has five cysteine residues, was found to contain 3.7 ± 0.2 free thiols per monomer. As previously reported, a small population (~10–20%) of wild-type CadC exists as a very stable disulfide crosslinked dimer when electrophoresed on a denaturing and reducing SDS-PAGE gel [12]. This species is refractory to reduction by tris(carboxyethyl)phosphine (TCEP) and other common reductants (data not shown). The stoichiometry of free thiols determined for each cysteine-substitution CadC mutant (each contain four cysteine residues) is as follows: C7G (2.7 ± 0.1), C11G (3.0 ± 0.1), C52G (2.7 ± 0.2), C58S (3.8 ± 0.2) and C60G (2.9 ± 0.2).

Bi(III) binding experiments

All metal binding experiments were carried out anaerobically at ambient temperature (~25 °C) using a Hewlett-Packard model 8452A spectrophotometer. For Bi(III) titrations, apo-CadC (0.8 mL of 40–50 μM) was diluted in an anaerobic glovebox with buffer T (10 mM Bis-Tris, 0.20 M NaCl, pH 7.0) and loaded into an anaerobic quartz cuvette. The cuvette was then fitted with a 250 μL adjustable volume Hamilton gas-tight syringe loaded with the Bi(III) titrant before removal from the anaerobic glovebox. Optical spectra of apo-CadC and of the protein after each addition of a known aliquot (5–20 μL) of Bi(III) titrant were collected from 190 to 1100 nm. Corrected spectra were obtained by first subtracting the apo-CadC spectrum from each metal-addition spectrum and then correcting each spectrum for dilution and the stoichiometry of Bi(III) bound per monomer [12]. For the Bi(III) displacement titration with Cd(II), 0.8 molar equivalents of Bi(III) was added anaerobically and allowed to incubate for 15 min at 25 °C, after which time the absorbance spectrum was taken. Cd(III) was then added in aliquots as described above, except the equilibration time was extended to 30 min following each addition of Cd(II). The data were corrected for dilution and background absorption. Titrations of a fixed concentration of Bi(III) with GSH, DTT or NAC were carried out in 10 mM Bis-Tris, 0.20 M NaCl, pH 7.0, where aliquots of GSH, NAC or DTT were added to 50–200 μM Bi(III) and allowed to equilibrate for 5–10 min before taking the absorbance spectrum. The data were corrected for background and dilution as described.

Analytical sedimentation equilibrium ultracentrifugation

All experiments were performed using a Beckman Optima XL-A analytical ultracentrifuge set to a speed of 35,000 rpm as described previously [12]. The ultracentrifuge cells were loaded anaerobically. Microcal Origin, a non-linear least-squares fitting program, was used to evaluate the sedimentation equilibrium data using a partial specific volume (v) of 0.724 mL/g and a solvent density (ρ) of 1.006 g/mL (calculated from the amino acid sequence and buffer composition). The data were fit to a self-association model of a single ideal species, assuming a monomer-dimer equilibrium characterized by the association constant K_a:

$$A_{r,total} = A_0 \exp\left[HM\left(x^2 - x_0^2\right)\right] + (A_0)^{n\,2} K_a \exp\left[HMn_2\left(x^2 - x_0^2\right)\right] + E \quad (1)$$

where A_r = absorbance at radius x, A_0 = absorbance at the reference radius x_0, H = constant $[(1-v\rho)\omega^2/2RT]$, M = monomer molecular weight, n_2 = number of monomers, K_a = association constant for the monomer-dimer equilibrium, and E = baseline offset. The values for M and K_a were optimized during the fit. The association constant was converted from absorbance to units of M^{-1} using the extinction coefficient $\epsilon_{280} = 6585\ M^{-1}\ cm^{-1}$ and a pathlength $l = 1.2$ cm.

Fluorescence anisotropy

All fluorescence anisotropy experiments were performed using an SLM 4800 spectrofluorometer fitted with polarizers in the L format, as described previously [12, 17]. The 34-mer, double-stranded *cad* O/P oligonucleotide (Operon Technologies) used was fluorescein-labeled on one 5′-end with the sequence given below:

F-5′-ATAATACACTCAAATAAATATTTGAATGAA-GATG-3′

3′-TATTATGTGAGTTTATTTATAAACTTACTTCTAC-5′

Apo-CadC or Bi_1-CadC (one equivalent Bi(III) per monomer) was titrated into 1.7 mL of 20 nM *cad* O/P at 25 ± 0.1 °C. The buffer used for the apo-CadC titration was 10 mM Bis-Tris, 0.40 M NaCl, 1 mM DTT, 50 μM EDTA, pH 7.0. For the Bi_1-CadC titrations of *cad* O/P, one mol equivalent of Bi(III) was added to apo-CadC (wild-type and cysteine-substitution mutants) anaerobically. The buffer used for the titration was 10 mM Bis-Tris, 0.40 M NaCl, 1 mM DTT, pH 7.0.

The polarization (P) and observed anisotropy (r) were calculated from:

$$P = \frac{\left(I_{VV} - \frac{I_{VH} I_{HV}}{I_{HH}}\right)}{\left(I_{VV} + \frac{I_{VH} I_{HV}}{I_{HH}}\right)} \quad (2)$$

and:

$$r = \frac{2P}{(3 - P)} \quad (3)$$

where I_{VV} and I_{VH} are the intensities of the emitted light polarized parallel and perpendicular, respectively, to the incident vertically polarized excitation beam. The factor I_{HV}/I_{HH} corrects the measured intensities for differences in the sensitivity of the detection of vertically and horizontally polarized emitted light. These data were fit, assuming a linear relationship between r_{obs} and fractional saturation of the DNA, to a dissociable dimer binding model in which dimeric CadC forms a 1:1 complex with the *cad* O/P oligonucleotide (defined by K_a) whose formation is linked to a CadC monomer-dimer equilibrium (defined by K_{dimer}) [12] using the program DynaFit [18]. The binding isotherms (raw r_{obs} versus $[CadC]_{total}$) were fit optimizing K_a and while holding K_{dimer} to the value determined independently for each of the apoproteins under similar solution conditions from sedimentation equilibrium ultracentrifugation experiments.

Results

Structural model of homodimeric CadC

Shown in Fig. 1 is a structural model of homodimeric CadC created by threading the CadC amino acid sequence through the X-ray crystallographic structure of apo-SmtB, a homologous zinc sensor from *Synechococcus* PCC7942. Plasmid pI258-encoded CadC contains five cysteine residues, three of which, Cys7 from the N-terminal "arm" and the Cys58/Cys60 pair from the α_3 helix of the helix-turn-helix DNA binding motif, are invariant. A fourth Cys, Cys11 in the N-terminal "arm", is largely conserved among functionally identified CadCs, while Cys52 in the α_2 helix is not conserved [14].

Bi(III) absorption spectroscopy of wild-type CadC

Shown in Fig. 2A are the apoprotein-subtracted absorption spectra resulting from a representative anaerobic Bi(III) titration of wild-type apo-CadC. The corresponding binding isotherm, presented as corrected ϵ_{265} ($M_{Bi}^{-1}\ cm^{-1}$) as a function of total Bi(III)/CadC

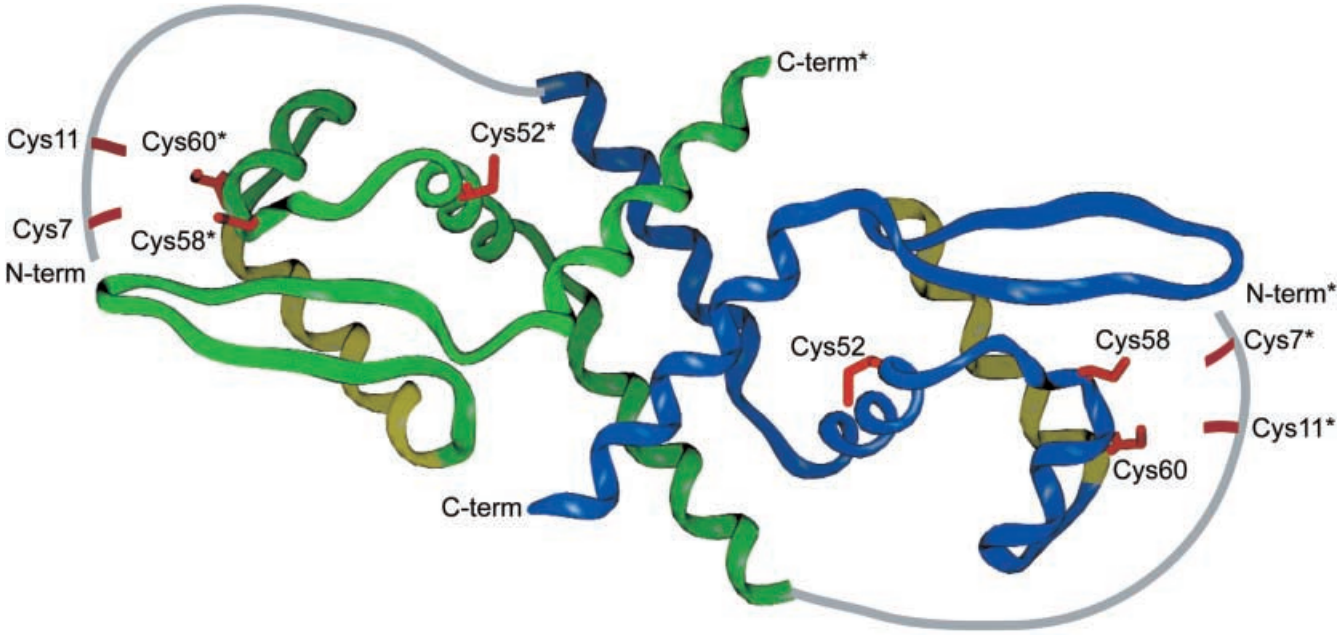

Fig. 1 Ribbon representation of a structural model of homodimeric *S. aureus* pI258 CadC (residues Thr27–Val118) based on the X-ray crystallographic structure of *Synechococcus* PCC7942 apo-SmtB [20] generated using Swiss-Model [19]. Since the N-terminal residues 1–20 of apo-SmtB were not observed in the crystal structure, threaded residues 1–26 and 119–122 of pI258 CadC are not present in the model. The N-terminal "arm" residues 1–26 are represented as a *gray* unstructured ribbon extending N-terminally from Thr27 in each of the two subunits (one in *green* and one in *blue*), with their positions speculative. The four conserved cysteine residues as well as Cys52 are colored *red*, with each of the putative recognition helices (α_R) shown in *yellow*. In this model, Cys58 and Cys60 are positioned in the –1 and +2 positions of the α_3 helix within the α_3-turn-α_R DNA-binding motif, while Cys7 and Cys11 are found in the N-terminal "arm". Residue numbers from the *green* subunit are numbered with an *asterisk*

monomer molar ratio, is shown in the inset. Over the course of this titration, a yellow-colored complex of Bi(III)-CadC is formed and results in three intense absorption maxima: a short wavelength absorbance band at 265 nm ($\epsilon_{265}\approx$35,000 M_{Bi}^{-1} cm^{-1}), a second absorption envelope at 350 nm ($\epsilon_{350}\approx$3000 M_{Bi}^{-1} cm^{-1}) and a third long-wavelength band centered at 415 nm ($\epsilon_{415}\approx$4000 M_{Bi}^{-1} cm^{-1}). The weak absorbance at 305 nm is attributed to Bi(III) binding to Bis-Tris, a chelating buffer used for these experiments (data not shown). Although there are very few published Bi(III) absorption spectra in the literature, these intense absorption bands can likely be assigned as $S^{-}\rightarrow$Bi(III) ligand-to-metal charge transfer (LMCT) transitions, since Bi(III) has a full d shell and is known to bind strongly to thiolate ligands [1].

The stoichiometry of binding is ~0.8 Bi(III) per CadC monomer, as determined by optical spectroscopy (Fig. 2A, inset), just like that previously determined for Cd(II) and Pb(II) [12]. Note that, under these conditions, CadC is fully dimeric [12]. This result seems most consistent with ~20% of CadC monomers inactivated as a result of partial cysteine oxidation (see Supplementary material). The binding curve, plotted as ϵ_{265} versus the Bi(III)/CadC monomer molar ratio (Fig. 2A, inset), appears to be characterized by two phases of ~0.4 molar equivalents of bound Bi(III) (solid line), since a fit of these data with a simple model which assumes a single class of Bi(III) binding sites on each CadC monomer appears to result in a poorer fit (dashed line). Although the structural origin of this is unknown, these data suggest that wild-type homodimeric apo-CadC as isolated may contain two distinct thiolate-containing sites, each characterized by slightly different molar absorptivities at 265 nm. This might arise from partial oxidation of Cys7, Cys11 and/or Cys58 in all preparations of CadC (see Supplementary material). In any case, the longest wavelength LMCT transition centered at 415 nm is a prominent feature throughout the Bi(III) titration.

The lowest energy LMCT transition positioned at 415 nm in the Bi(III)-CadC absorption spectrum is most consistent with a Bi(III) complex containing four thiolate ligands, owing to the strong correspondence of this absorption band with that obtained for the tetradentate [$Bi(DTT)_2$] complex, which is also yellow in color and saturates at a stoichiometry consistent with S_4 coordination (Fig. 2B). In contrast, all structurally characterized trithiolato (S_3) coordination complexes are characterized by a long-wavelength absorption band at 350 nm, i.e., shifted to significantly higher energy [5]. These include the $Bi(III)_7$-metallothionein complex ($\epsilon_{350}\approx$2100 M^{-1} cm^{-1} per Bi(III) bound), in which each Bi(III) ion is coordinated strongly to just three cysteine ligands, as well as Bi(III)-saturated GSH and NAC, which form [$Bi(GSH)_3$] and [$Bi(NAC)_3$] as determined by X-ray absorption spectroscopy [5]. Like Bi-MT, the absorption spectra of [$Bi(GSH)_3$] and [$Bi(NAC)_3$] are characterized by absorption maxima at ~350 nm and are colorless (Fig. 2B) [5], as is the Bi(III) complex of β-mercaptoethanol (β-ME) (data not shown). These

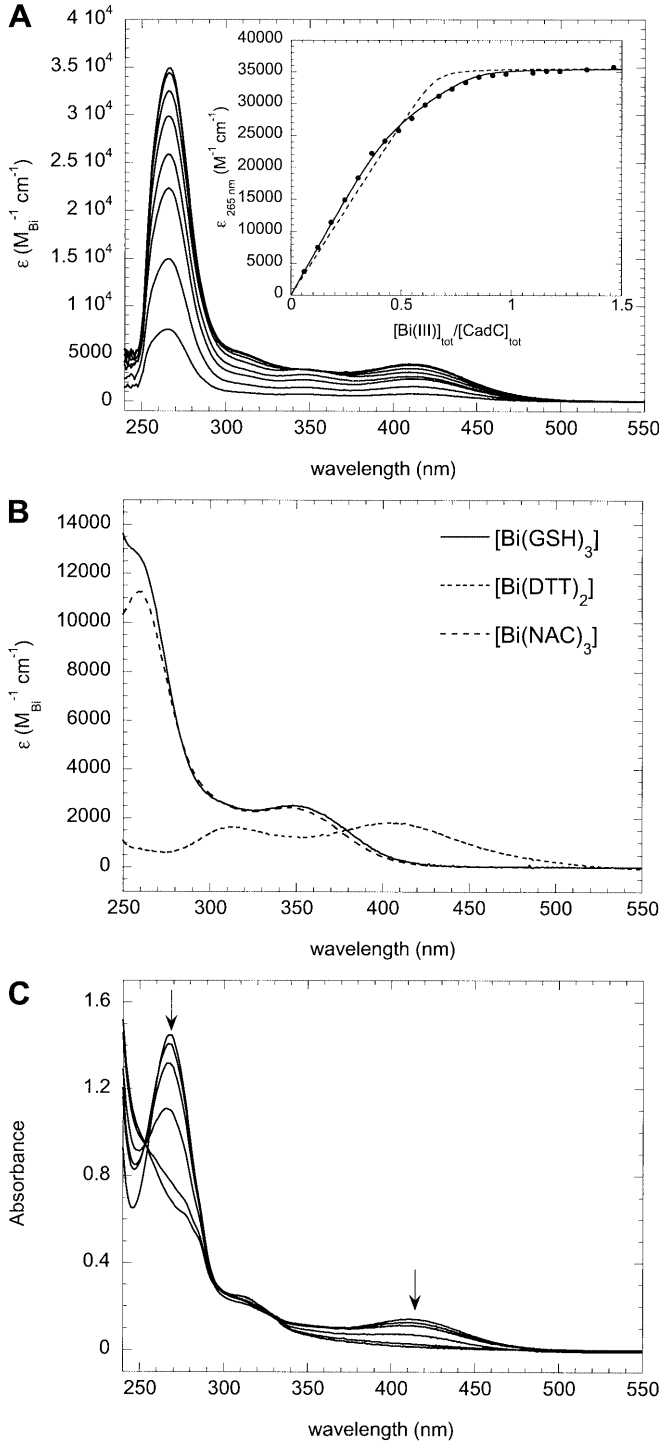

Fig. 2A–C Bi(III) titration of apo wild-type CadC. **A** Apo-subtracted difference absorption spectrum of 47.0 μM apo-CadC titrated anaerobically with a Bi(III) stock solution. Conditions: 10 mM Bis-Tris, 0.20 M NaCl, pH 7.0, 25 °C. *Inset*: corresponding Bi(III) binding isotherm of the titration at 265 nm. The *dashed line* represents a fit to a 1: 1 Bi(III) per CadC monomer binding model where active [CadC] = 37.6 μM and $K_{Bi} = 9.9(\pm 9)\times10^6$ M^{-1}. The *solid line* represents a fit to a model which assumes a maximum 1:1 Bi(III):monomer stoichiometry, but with two spectroscopically distinguishable sites (each with a stoichiometry of 0.5), where active [CadC] = 37.6 μM and $K_{Bi} = 1.6(\pm 1.0)\times10^7$ M^{-1} in each case. Note that these K_{Bi} are meaningless and are shown for illustration only (see text for details), since, under these conditions, K_{Bi} is too large to accurately measure at this [CadC]. **B** Saturated $[Bi(GSH)_3]$, $[Bi(NAC)_3]$ and $[Bi(DTT)_2]$ absorption spectra. Conditions: 10 mM Bis-Tris, 0.20 M NaCl, pH 7.0, 25 °C, containing 50 μM (GSH and DTT titrations) or 200 μM (NAC titration) Bi(III) ion. The stoichiometric point for the Bi(III)-DTT titration was found to be 2.1 ± 0.1 DTT per Bi(III) ion in two separate experiments. **C** Absorption spectra obtained as a result from an anaerobic Cd(II) titration of 50 μM CadC with 0.8 equiv of Bi(III) bound. Data were corrected as described (see Materials and methods). Conditions: 10 mM Bis-Tris, 0.20 M NaCl, pH 7.0, 25 °C

spectral observations are fully consistent with the expectation that LMCT transitions will move to lower energies (longer wavelengths) as the number of thiolate ligands that coordinate the metal increases [21, 22, 23, 24]. These model compound spectra, coupled with spectroscopic characterization of the cysteine substitution mutants (see below), support our proposal of a primary S_4 coordination complex on fully reduced homodimeric wild-type CadC, with some non-native S_3 complex also present, formed as a result of partial oxidation of cysteine residues on CadC as isolated (see Supplementary material).

Shown in Fig. 2C are the full absorbance spectra which result from a representative titration of Cd(II) into the Bi(III)-saturated CadC complex. The decrease in the $S^-\rightarrow$Bi(III) LMCT at 415 nm in this experiment reveals that stoichiometric Cd(II) per CadC monomer efficiently displaces all of the bound Bi(III). A concomitant increase in absorbance at 240 nm was observed as expected from $S^-\rightarrow$Cd(II) LMCT [12], indicating that CadC is binding Cd(II); however, at the concentrations used for the titrations the absorbance was well out of the linear range. The affinity of the tetrathiolate Cd(II) site of CadC was determined previously ($K_{Cd}\approx4\times10^{12}$ M^{-1}) [12]; since stoichiometric Cd(II) displaces Bi(III), a value of $K_{Bi} \leq 10^{12}$ M^{-1} can be estimated from these data.

Bi(III) absorption spectroscopy of Cys→Gly CadC mutants

To determine which cysteine residues are involved in the direct coordination of Bi(III), a series of cysteine substitution mutants of CadC were characterized by Bi(III) absorption spectroscopy. Shown in Fig. 3 are the corrected molar absorptivity spectra of the Bi(III)-saturated cysteine substitution mutants of CadC. Relative to wild-type CadC, the longest wavelength absorption transition for C7G, C11G and C60G CadCs was found to move to significantly higher energy, to a spectral region fully compatible with coordination by three rather than four thiolate ligands. For example, substitution of Cys60 in C60G CadC gives rise to a significant blue shift of the long-wavelength LMCT to 355 nm ($\epsilon_{355}\approx3000$ M_{Bi}^{-1} cm^{-1}) and a slight shift in the short-wavelength transition to 260 nm with a concomitant decrease in molar absorptivity ($\epsilon_{260nm}\approx14{,}000$ M_{Bi}^{-1} cm^{-1}). A very similar

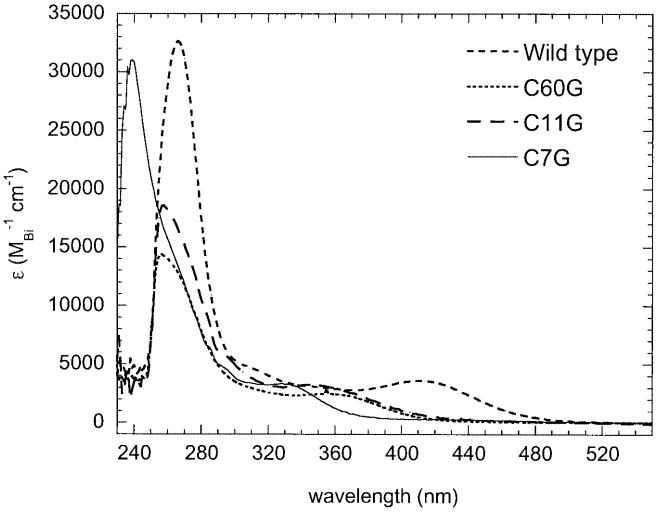

Fig. 3 Bi(III) absorption spectra of saturated wild-type, C7G, C11G and C60G CadCs. Apoprotein-subtracted difference spectra of Bi(III)-saturated CadC proteins expressed per mole Bi(III) bound: wild-type (*medium dashes*), C7G (*solid line*), C11G (*long dashes*) and C60G (*short dashes*)

absorption spectrum characterizes C11G CadC, revealing that Cys11, like Cys60, donates a coordination bond to the Bi(III) ion. Interestingly, substitution of Cys7 has a more pronounced effect on the Bi(III) absorption spectrum since the near-UV LMCT has shifted to 333 nm ($\epsilon_{333}\approx$4000 M_{Bi}^{-1} cm^{-1}), with the higher energy charge transfer band strongly blue shifted to 238 nm ($\epsilon_{238}\approx$31,000 M_{Bi}^{-1} cm^{-1}). This might indicate a more marked perturbation of the coordination geometry for the bound Bi(III) ion in this mutant upon the loss of this cysteine ligand. Cys58 also appears to be crucial to the stability of the Bi(III)-CadC complex, since titration of C58S CadC with Bi(III) leads to immediate precipitation of the protein over a wide range of solution conditions (data not shown). As expected from functional studies and a lack of conservation among CadCs [14], the Bi(III) optical spectrum for C52G CadC is essentially indistinguishable from wild-type CadC ($\epsilon_{415}\approx$3800 M_{Bi}^{-1} cm^{-1}; $\epsilon_{268}\approx$34,000 M_{Bi}^{-1} cm^{-1}) and is therefore not a ligand to the metal (spectrum not shown). Taken together, these spectroscopic data show that Bi(III) forms a tetrathiolate coordination complex in wild-type CadC utilizing Cys7 and Cys11 from the N-terminal "arm" and Cys58 and Cys60 from the α_3 helix (cf. Fig. 1). It is not known with certainty as yet if these two pairs of ligands (7/11 and 58/60) are derived from the same or different monomers in homodimeric CadC, although it seems most likely they come from different monomers.

Bi(III)-dependent allosteric regulation of *cad* O/P binding

Since wild-type CadC and all cysteine substitution mutants form stable coordination complexes with Bi(III) (with the exception of C58S CadC), it was next of interest to examine to what extent Bi(III) binding modulates *cad* O/P binding affinity. Fluorescence anisotropy experiments were performed using a 5′-fluorescein-labeled 34 base pair oligonucleotide that contains the region of the *cad* O/P that was protected by CadC in footprinting experiments [11]. Previous fluorescence anisotropy experiments showed that apo-CadC binds to the 34-bp *cad* O/P oligonucleotide with a high affinity ($K_a = 1.1\times10^9$ M^{-1}) under conditions of relatively high salt concentration (0.40 M NaCl, pH 7.0, 25 °C), which is strongly negatively regulated upon binding of stoichiometric Pb(II) or Cd(II) [12].

Representative fluorescence anisotropy-based binding isotherms of wild-type apo-CadC and CadC with one equivalent of Bi(III) per monomer (Bi_1-CadC) with the fluorescein-labeled *cad* O/P oligonucleotide are shown in Fig. 4A. The solid and dashed lines through each data set represent a fit to a dissociable dimer model assuming a 1:1 CadC dimer/DNA complex with the dimerization constant fixed at $K_{dimer} = 3\times10^6$ M^{-1} (Table 1), as determined by analytical equilibrium ultracentrifugation [12]. The intrinsic DNA binding affinities (K_a) (Table 2) resolved from multiple independent experiments incorporate the linkage of DNA binding by dimeric CadC to the CadC monomer-dimer equilibrium defined by K_{dimer}. Quantitative analysis of the data reveal that the addition of one equivalent of Bi(III) per CadC monomer decreases K_a by 165-fold relative to apo-CadC. This is direct evidence that Bi(III) binding to wild-type CadC results in strong negative regulation of specific DNA binding (Table 2).

Figure 4B and Fig. 4C present representative binding isotherms obtained for two of the CadC cysteine substitution mutants as apoproteins (solid symbols) or when complexed to Bi(III) (open symbols). The solid and dashed lines through the experimental data sets are the best fits to the dissociable dimer model with the K_{dimer} fixed at the values given in Table 1. For C60G CadC (Fig. 4B), the apoprotein titration is indicative of high affinity binding to the *cad* O/P oligonucleotide [$K_a = 1.0(\pm0.6)\times10^9$ M^{-1}]. Strikingly, the identical experiment carried out with Bi_1-C60G CadC reveals complete loss of allosteric regulation of DNA binding by Bi(III) [$K_a = 1.0(\pm0.1)\times10^9$ M^{-1}]. Apo-C7G CadC is characterized by the same high affinity for the *cad* O/P DNA as wild-type CadC [$K_a = 8.3(\pm0.6)\times10^8$ M^{-1}]. The binding of stoichiometric Bi(III) to C7G CadC effects only a small decrease (~10-fold) in the affinity of the repressor for the *cad* O/P; this suggests that Cys7 is also critical for Bi(III)-mediated negative regulation (Fig. 4C). The best fit value for the anisotropy binding isotherm for apo-C11G CadC gives $K_a = 5.8(\pm0.5)\times10^8$ M^{-1} (Table 2). Interestingly, K_{dimer} for C11G CadC is ~16-fold lower than that for wild-type CadC, indicating that this mutation also negatively influences the dimerization equilibrium (Table 1). K_a decreases ~28-fold for Bi_1-C11G CadC relative to the apoprotein, which suggests that Cys11, like Cys7, is required for full negative regulation of DNA binding, although it is clearly not as critical. As

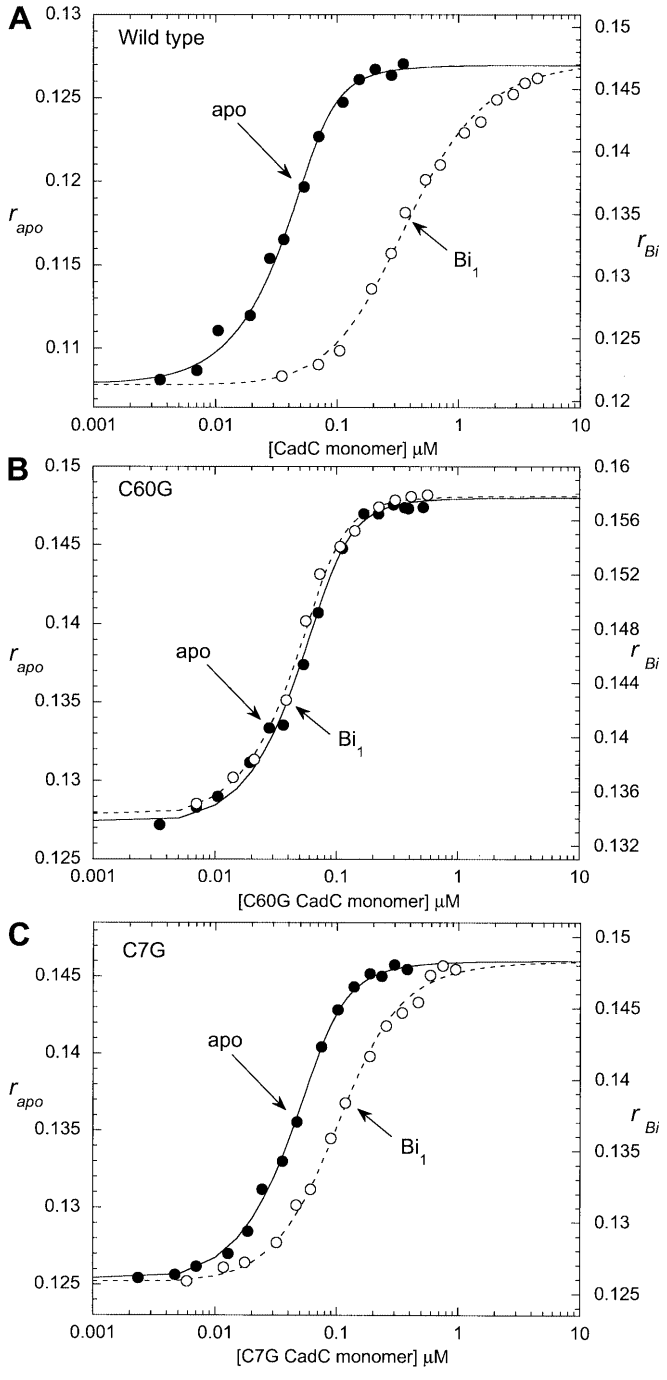

◀

Fig. 4A–C Fluorescence anisotropy titrations of the *cad* O/P oligonucleotide with the apo and Bi_1 forms of wild-type and Cys→Gly CadC mutants. **A** Shown are representative binding isotherms (r_{obs} versus $[CadC]_{total}$) generated from titrations of 5′-fluorescein-labeled *cad* O/P with apo-CadC (*filled circles*) or Bi_1-CadC (*open circles*). Conditions: 10 mM Bis-Tris, 0.40 M NaCl, 1 mM DTT, 50 μM EDTA (EDTA not present in the Bi_1-CadC titration), pH 7.0, 25 °C. The *solid* and *dashed lines* through the data sets represent the best fits to a dissociable dimer model that assumes a 1:1 dimer-DNA complex for the titration, with K_{dimer} fixed at 3×10^6 M^{-1}. For the apo-CadC titration, $K_a = 1.1(\pm0.2)\times10^9$ M^{-1}, and for the Bi_1-CadC titration, $K_a = 6.7(\pm0.6)\times10^6$ M^{-1}. **B** Shown is a representative binding isotherm obtained from a titration of *cad* O/P DNA with apo-C60G CadC (*filled circles*) or Bi_1-C60G CadC (*open circles*) at 25 °C. The *solid* and *dashed lines* through the data sets represent the best fits to a dissociable dimer model (described above) with K_{dimer} fixed at 1×10^6 M^{-1} (Table 1). $K_a = 1.0(\pm0.6)\times10^9$ M^{-1} for the apo-C60G titration, while $K_a = 1.0(\pm0.1)\times10^9$ M^{-1} for the Bi_1-C60G titration. **C** Shown is a representative binding isotherm obtained from a titration of *cad* O/P DNA with apo-C7G CadC (*filled circles*) or Bi_1-C7G CadC (*open circles*). The *solid* and *dashed lines* through the data are the best fits to a dissociable dimer model where K_{dimer} is fixed at 2.8×10^6 M^{-1} (Table 1). For the apo-C7G titration, $K_a = 8.3(\pm0.6)\times10^8$ M^{-1}, while for the apo-C7G titration, $K_a = 7.2(\pm0.9)\times10^7$ M^{-1}

Table 1 Sedimentation equilibrium ultracentrifugation of wild-type and mutant CadC proteins

CadC[a]	Molecular mass (g/mol)	K_{dimer}[b] (M^{-1})
Wild-type[c]	13,754(±154)	$3.0(\pm2.0)\times10^6$
C7G	14,001(±544)	$2.8(\pm0.4)\times10^6$
C11G	13,832(±228)	$1.8(\pm0.2)\times10^5$
C60G	13,882(±339)	$1.0(\pm0.5)\times10^6$
C52G	13,991(±410)	$2.8(\pm0.6)\times10^6$

[a]Conditions: 5 mM MES, 0.20 M NaCl, 2 mM DTT, 1 mM EDTA, pH 7.0, 25 °C
[b]The dimerization constant determined from the best fit of the experimental data to a monomer-dimer equilibrium model with the optimized monomer molecular mass. The expected molecular mass is 13,779 g/mol for wild-type CadC and 13,732 g/mol for all Cys→Gly CadC mutants (see Materials and methods)
[c]From ref. [12]

Table 2 The affinities of apo- and Bi_1-CadC proteins for the *cad* O/P oligonucleotide

CadC	K_a (M^{-1})[a] apo	K_a (M^{-1})[b] Bi_1	Fold decrease relative to apo
Wild-type	$1.1(\pm0.2)\times10^9$	$6.7(\pm0.6)\times10^6$	165
C7G	$8.3(\pm0.6)\times10^8$	$7.2(\pm0.9)\times10^7$	11
C11G	$5.8(\pm0.5)\times10^8$	$2.1(\pm0.4)\times10^7$	28
C52G	$1.0(\pm0.3)\times10^9$	$7.3(\pm0.8)\times10^6$	137
C60G	$1.0(\pm0.6)\times10^9$	$1.0(\pm0.1)\times10^9$	1

[a]Conditions: 10 mM Bis-Tris (or 5 mM MES), 0.40 M NaCl, 1 mM DTT, 50 μM EDTA, pH 7.0, 25 °C
[b]Conditions: 10 mM Bis-Tris, 0.40 M NaCl, 1 mM DTT, pH 7.0, 25 °C. Titrations were performed with the concentration of *cad* O/P fixed (20 nM) and apo-CadC or Bi_1-CadC (one equivalent of Bi(III) bound per monomer) titrated. Binding isotherms were fit for K_a to a dissociable dimer model described by a 1:1 CadC dimer-DNA complex that is linked to a monomer-dimer equilibrium and the value reported is the average of three separate experiments. The dimerization constants for each protein were fixed during the fit to the values listed in Table 1

expected from the spectroscopic results, apo-C52G CadC exhibits wild-type affinity for the *cad* O/P fragment and is characterized by full negative regulation of DNA binding by the direct binding of Bi(III) (Table 2).

Discussion

S. aureus pI258 CadC has previously been shown to bind Cd(II) and Pb(II) through coordination by cysteine thiolate ligands and that binding of these regulatory metals results in a significant decrease in the affinity of

the metallated protein for the *cad* O/P oligonucleotide, thus providing a model for de-repression [12]. This is consistent with in vivo reporter gene fusion assays in the native host, *S. aureus*, which showed that expression from the *cad* O/P is de-repressed upon addition of Cd(II) and Pb(II) to the growth media [7]. Another report suggests that Bi(III) also induces the release of CadC from the *cad* O/P [11]. In this paper, the stoichiometry, relative affinity and coordination chemistry of the Bi(III) site of CadC is reported. In addition, it is shown that Bi(III) binding strongly allosterically regulates *cad* O/P DNA binding in vitro.

The Bi(III) optical absorption spectroscopy of wild-type and mutant CadCs, coupled with comparison to several small molecule Bi(III) coordination complexes {$[Bi(GSH)_3]$, $[Bi(\beta ME)_3]$, $[Bi(NAC)_3]$, $[Bi(DTT)_2]$}, is most consistent with a coordination model in which four cysteine residues (Cys7, Cys11, Cys58 and Cys60) provide direct coordination bonds to the bound Bi(III) ion in fully reduced CadC. The actual optical spectrum of wild-type CadC suggests the presence of a mixture of Bi(III) complexes (Fig. 2A), likely a population of S_3 and S_4 sites with the S_3 site arising from partial oxidation of the protein (Fig. 1; Supplementary material). Consistent with this, the Bi(III) optical spectrum of a preparation of CadC that contains ~2.5 free thiols per CadC monomer (out of five cysteine residues) is characterized only by weak absorption at 350 nm, with no evidence for the long-wavelength 415 nm transition diagnostic of S_4 coordination (data not shown). In addition, the fact that Cd(II) quantitatively displaces Bi(III) from Bi_1-CadC (Fig. 2C) is consistent with the hypothesis that Cd(II) and Bi(III) share the same cysteine ligands and that CadC has a lower affinity for Bi(III) than Cd(II).

Finally, we show that the binding of one molar equivalent of Bi(III) to apo-CadC induces strong allosteric regulation of *cad* O/P DNA binding (Fig. 4A). The DNA binding isotherms are well described by a model which links DNA binding affinity to a monomer-dimer equilibrium, where K_{dimer} is fixed to the value determined from sedimentation equilibrium ultracentrifugation (Table 1) [12]. Apo-CadC binds to a *cad* O/P oligonucleotide that contains the specific binding site for CadC, as defined by in vitro footprinting experiments, with an affinity on the order of 10^9 M^{-1}, in a solution containing relatively high monovalent salt concentration (0.40 M NaCl) [11, 12]. Under the same conditions, CadC with one equivalent of Bi(III) binds ~165-fold weaker than does the metal-free form of the protein (Fig. 4A, Table 2). In previous experiments, the Cd(II) and Pb(II) forms of CadC were shown to bind with a 250- to 340-fold decrease in the K_a relative to apo CadC [12]. From these functional results it appears that negative regulation of *cad* O/P binding is stronger for Cd(II) and Pb(II) than it is for Bi(III), although the results for all three metals are of the same order of magnitude. This result is corroborated by in vitro gel mobility shift assays, which reveal that Cd(II), Pb(II) and Bi(III) cause at least partial dissociation of CadC from a 203-bp *cad* O/P containing DNA fragment [11]. These results are consistent with a model where the metal-free form of CadC associates specifically and with high affinity to the *cad* O/P to repress transcription of the operon. In response to the direct binding of sensing regulatory metals such as Cd(II), Pb(II) and Bi(III) to cysteine thiolates in the N-terminal "arm" and α_3 helix, the DNA binding affinity is significantly reduced which enables RNA polymerase to access the promoter, leading to de-repression of transcription and the expression of the gene encoding the CadA efflux pump.

Functionally, loss of Cys60 is clearly the most detrimental to allosteric regulation of DNA binding by Bi(III) (Fig. 4B). C60G CadC is no longer able to "sense" Bi(III), despite the fact that, by optical spectroscopy, Bi(III) forms a stable complex with C60G CadC (Fig. 3). Both Cys7 and Cys 11 are also required for full negative regulation at the *cad* O/P (Fig. 4, Table 2), with the presence of Cys7 more critical than that of Cys11. These findings are consistent with the conservation of specific cysteine residues in CadC with Cys7, Cys58 and Cys60 absolutely conserved in all known functional CadCs and with Cys11 only largely conserved [14]. Although the mechanism for allosteric regulation is not known, binding of Bi(III) to Cys58 and Cys60 in the conserved $E^{56}LCVCD^{61}$ region (which overlaps the α_3 helix) [14, 25] and to Cys7 and Cys11 in the N-terminal "arm" (Fig. 1), together, may induce a conformational change in the α_3 helix of the α_3 helix-turn-α_R helix DNA binding motif which affects the recognition helix (α_R), thus disrupting protein-DNA interactions. Further structural studies are required to determine the molecular basis for allosteric regulation of DNA binding by Bi(III), compared to other inducing metal ions, and, in particular, how Cys60 functions to play such a critical role in this process.

Acknowledgements We thank Dr. Simon Silver at the University of Illinois at Chicago for his gift of a plasmid encoding wild-type *S. aureus* pI258 *cadC* gene, from which overexpression plasmids were prepared, and Dr. Barry Rosen at Wayne State University for kindly providing the overexpression plasmids encoding the cysteine substitution mutants of CadC. This work is supported by grants from the NIH (GM42569) and the Robert A. Welch Foundation (A-1295).

References

1. Sadler PJ, Li HY, Sun HZ (1999) Coord Chem Rev 186:689–709
2. Asatoa E, Akaminea Y, Nukadab R, Mikuriyab M, Deguchic S, Yokotac Y (1997) J Inorg Biochem 67:146
3. Roine RP, Salmela KS, Hook-Nikanne J, Kosunen TU, Salaspuro M (1992) Life Sci 51:195–200
4. DiSilvestro RA, Liu J, Klaassen CD (1996) Res Commun Mol Pathol Pharmacol 93:163–170
5. Sun H, Li H, Harvey I, Sadler PJ (1999) J Biol Chem 274:29094–29101
6. Sun H, Li H, Mason AB, Woodworth RC, Sadler PJ (2001) J Biol Chem 276:8829–8835
7. Yoon KP, Misra TK, Silver S (1991) J Bacteriol 173:7643–7649

8. Rensing C, Sun Y, Mitra B, Rosen BP (1998) J Biol Chem 273:32614–32617
9. Wu J, Rosen BP (1993) J Biol Chem 268:52–58
10. Rosen BP (1996) J Biol Inorg Chem 1:273–277
11. Endo G, Silver S (1995) J Bacteriol 177:4437–4441
12. Busenlehner LS, Cosper NJ, Scott RA, Rosen BP, Wong MD, Giedroc DP (2001) Biochemistry 40:4426–4436
13. Lippard S, Berg J (1994) Principles of bioinorganic chemistry. University Science Books, Mill Valley, Calif., pp 21–24
14. Sun Y, Wong MD, Rosen BP (2001) J Biol Chem 276:14955–14960
15. Pace CN, Vajdos F, Fee L, Grimsley G, Gray T (1995) Protein Sci 4:2411–2423
16. Guo J, Giedroc DP (1997) Biochemistry 36:730–742
17. Chen X, Agarwal A, Giedroc DP (1998) Biochemistry 37:11152–11161
18. Kuzmic P (1996) Anal Biochem 237:260–273
19. Peitsch MC (1996) Biochem Soc Trans 24:274–279
20. Cook WJ, Kar SR, Taylor KB, Hall LM (1998) J Mol Biol 275:337–346
21. Payne JC, ter Horst MA, Godwin HA (1999) J Am Chem Soc 121:6850–6855
22. Chen X, Chu M, Giedroc DP (2000) J Biol Inorg Chem 5:93–101
23. Pountney DL, Tiwari RP, Egan JB (1997) Protein Sci 6:892–902
24. Henehan CJ, Pountney DL, Zerbe O, Vasák M (1993) Protein Sci 2:1756–1764
25. Shi W, Wu J, Rosen BP (1994) J Biol Chem 269:19826–19829